ELECTRON BEAM COLLIMATION FOR SLICE DIAGNOSTICS AND GENERATION OF FEMTOSECOND SOFT X-RAY PULSES FROM A FREE ELECTRON LASER*

S. Di Mitri#, M. Bossi, D. Castronovo, I. Cudin, M. Ferianis, L. Fröhlich, Elettra-Sincrotrone Trieste S.C.p.A., Basovizza (TS), Italy

Abstract

We present the experimental results of femtosecond slicing an ultra-relativistic, high brightness electron beam with a collimator [1]. We demonstrate that the collimation process preserves the slice beam quality, in agreement with our theoretical expectations, and that the collimation is compatible with the operation of a linear accelerator. Thus, it turns out to be a more compact and cheaper solution for electron slice diagnostics than commonly used radiofrequency deflecting cavities and having minimal impact on the machine design. The collimated beam can also be used for the generation of stable femtosecond soft x-ray pulses of tunable duration from a free electron laser.

ELECTRON SLICING WITH A COLLIMATOR

The feasibility and operability of the electron beam collimation at ultra-relativistic energies for slice diagnostics was investigated in the radiofrequency linear accelerator (RF linac) of FERMI@Elettra FEL [2, 3]. The collimator is a horizontal scraper made of two identical, cylindrical and individually movable rods of copper. The rod diameter is 13 mm wide.

Collimation for slice diagnostics was applied to an initial 350 pC, 5 ps FWHM long beam. The magnetic chicane and the upstream linac were set in order to define the bunch length compression by a factor 5.5. All the relevant beam and machine parameters adopted in the experiment are listed in Table 1. The geometric beam size in the middle of BC1 was $\sigma_\beta = 160$ μm so, following the prescription in [4], Eq.1, the scraper blades were inserted into the vacuum chamber to define a half-aperture at least three times bigger, namely 0.5 mm wide. The chromatic beam size σ_x = 2.6 mm, that is the product of the energy dispersion function and the fractional energy spread rms, was much larger than the geometric one, so we can use Eq.1 to evaluate the duration of the collimated beam that is $\Delta t_{col} \approx 70$ fs FWHM. The charge of such a beam is expected to be $Q_{col} = Q_i \dfrac{C\Delta t_{col}}{\Delta t_i} \approx 27\,pC$, where Q_i and Δt_i are, respectively, the initial total charge and the initial bunch duration (FWHM) and C is the compression factor. The scraper aperture was consecutively translated to select 12 longitudinal slices of the bunch. Each slice was accelerated and transported to the linac end, in the so-called TLS region. The slice optical parameters were measured both in the BC1 and in the TLS region with the quadrupole scan technique [5, 6], in dedicated diagnostic stations.

COLLIMATOR'S GEOMETRIC TRANSVERSE WAKEFIELD

The impact of the scraper transverse wakefield on the emittance of the collimated beam was analytically estimated, with the limitation that the model starts failing when the particles travel at a distance comparable to the collimator half-aperture. Following [7], the FERMI scraper behaves like a flat, long collimator and the kick factor κ must be computed in the diffractive regime. For a half-aperture 0.5 mm wide, we have κ = 72 V/pC/mm. This is a rather large value but its effect on the emittance is mitigated by the low charge traversing the scraper and a proper optics setting at the collimator location. In the case of a 50pC beam charge traveling 0.4 mm far from the scraper axis, the collimator's kick is [7] $\theta = \dfrac{hQ\kappa}{E} = 4.8\mu rad$, where Q is the bunch charge, h is the bunch centroid distance from the collimator axis, κ is the kick factor in the plane of interest and E is the beam mean energy. Following [8], the normalized emittance growth can be estimated with:

$$\gamma\varepsilon_x = \gamma\sqrt{\varepsilon_{x,0}^2\left(1+\frac{\beta_x}{\varepsilon_{x,0}}\theta^2\right)} \le 0.07\mu m, \qquad (1)$$

where γ is the relativistic Lorentz factor, $\gamma\varepsilon_{x,0} \approx 1$ μm is the unperturbed RMS geometric emittance and β_x is the horizontal betatron function at the collimator location. Its design value for a matched beam is 3m. In Eq.1, we considered the case of a reasonably mismatched beam, *i.e.* β_x = 10m. We do not expect any effect in the vertical plane because the collimator has no aperture restrictions in that plane.

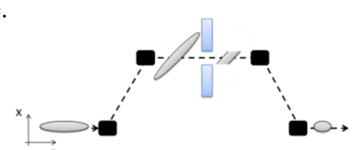

Figure 1: Schematic top view (not to scale) of electron slicing with a collimator placed in the middle of a magnetic chicane, once a linear energy chirp is imparted to the electron beam by an upstream accelerator. Published in [1].

*Work supported in part by the Italian Ministry of University and Research under grants FIRB-RBAP045JF2 and FIRB-RBAP06AWK3
#simone.dimitri@elettra.eu

ISBN 978-3-95450-127-4

SLICE EMITTANCE MEASUREMENT

Figures 2–4 show the slice distribution of the charge, the emittance and the Courant-Snyder (C-S) parameters [9] measured in BC1 and in TLS. The quadrupole scan technique and measurement accuracy are discussed, *e.g.*, in [6]. The largest error bars for the emittance measurement are dominated by the variation of the central value over several consecutive measurements. This variation is mainly addressed to imperfect background subtraction during the beam image recording. The maximum error over all measurements is considered for the C-S- parameters. By comparing the optics parameters of the entire beam, listed in Table 1, with those of Figures 2–4 , we infer that the slice emittance after collimation is typically equal or smaller than that of the whole beam, and that the scraper wakefield does not degrade the emittance of the collimated beam. Moreover, the slice emittance is approximately preserved during the beam transport from BC1 to TLS, while the projected emittance in TLS is larger than in BC1. This is an indication that it is dominated by the correlation of the slices' centroid coordinates in the transverse phase space, such as those induced by linac geometric wakefields [10].

Table 1: Electron beam and machine parameters used during beam collimation for slice diagnostics. The optical parameters were measured at the entrance of the quadrupole used for the emittance measurement.

Parameter	In BC1	In TLS	Units
Charge	350	10 – 35	pC
Mean energy	303	1205	MeV
Energy spread, RMS	1.0	0.3	%
Norm. projected emittance, RMS	1.7 (H), 1.3 (V)	3.7 (H), 1.9 (V)	mm mrad
β-function	22.2 (H), 24.1 (V)	9.4 (H), 8.2 (V)	m
α-function	9.3 (H), -3.1 (V)	4.5 (H), -3.9 (V)	
Dipole bending angle	85		mrad
Central momentum dispersion	255		mm
Compression factor	5.5		

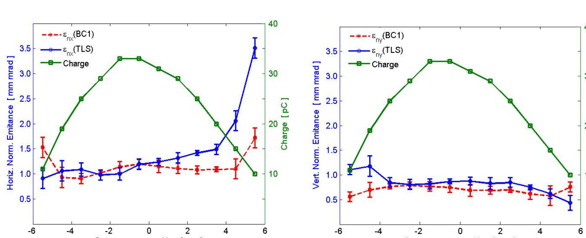

Figure 2: Charge (squares) and slice normalized emittance measured in the FERMI BC1 (dots, dashed line) and TLS (dots, solid line) linac regions. Left plot is for the horizontal plane, right for the vertical. Published in [1].

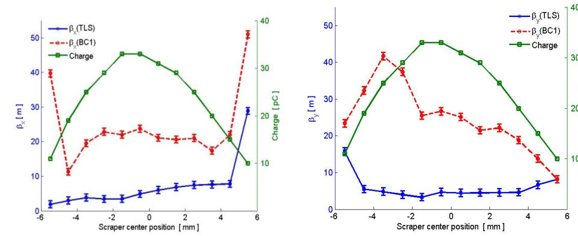

Figure 3: Charge (squares) and slice β-function measured in the FERMI BC1 (dots, dashed line) and TLS (dots, solid line) linac regions. From left to right:, , α-function. Left plot is for the horizontal plane, right for the vertical. Published in [1].

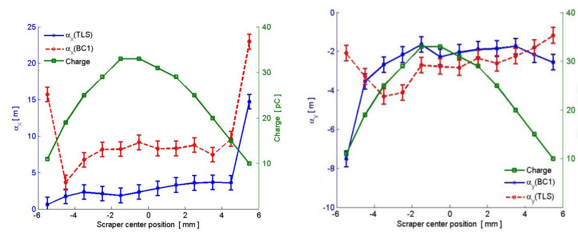

Figure 4: Charge (squares) and slice α-function measured in the FERMI BC1 (dots, dashed line) and TLS (dots, solid line) linac regions. Left plot is for the horizontal plane, right for the vertical. Published in [1].

FEL SIMULATION WITH SLICED BEAM

We simulated the FERMI high gain harmonic generation [3, 11, 12] with the code PERSEO [13]. The undulator line consists of one longer period undulator (called modulator) for electron beam and seed laser interaction, a dispersive section (R_{56}=-40 μm) for bunching enhancement and six identical shorter period undulators (called radiators) in the planar horizontal configuration. The seed laser delivers 100 MW of peak power at 266 nm wavelength in a flat, 350 fs long pulse. The radiators are tuned to the 10^{th} harmonic of the seed laser, i.e. to a wavelength of 26.6 nm. We chose electron beam parameters that reflect the most recent FERMI performance [2]: a 500 pC, 10 ps long electron beam is assumed to be compressed by a factor 15 in BC1 to achieve a flat current profile of approximately 750 A, and accelerated to the energy of 1.2 GeV. The final slice emittance is 1.0 mm mrad and the slice energy spread is 150 keV. We assume the collimator setting adopted for the aforementioned slice diagnostics experiment. The FWHM duration of the collimated beam turns out to be [4] $\Delta t_{col} \approx 110$ fs, carrying a charge $Q_{col} \approx 80\,pC$. We note that Δt_{col} and Q_{col} scale as $\sqrt{\beta_x}$ in the middle of the chicane, *i.e.* a ten times smaller β_x would allow the generation of a 25 pC, 35 fs long collimated beam. The FEL power emitted by the 80 pC bunch along the undulator is shown in Figure 5. The final peak power is 3 GW over 38 fs (FWHM), which corresponds to ≈$2\cdot10^{13}$ photons/pulse. The final FEL pulse duration is also shown as a function of the collimator half-aperture in BC1. The maximum peak power decreases from 3.71 to 2.98 GW

ISBN 978-3-95450-127-4

(not shown) as the photon pulse shrinks from 120 to 16 fs (FWHM).

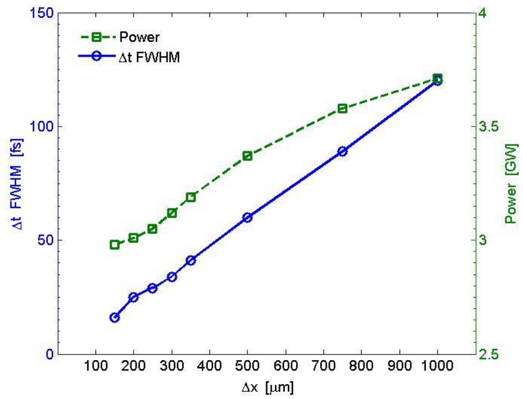

Figure 5: FERMI FEL final pulse duration FWHM (solid line) and peak power (dashed line) versus the collimator half-aperture. Simulations were performed with the code PERSEO. Published in [1].

DISCUSSION

Beam collimation for slice diagnostics can be applied to transverse dynamics, as shown in this article, and to the longitudinal, as reported in the Appendix of [6]. In contrast to slice diagnostics performed with RF deflectors, which preserve the entire beam structure, beam collimation isolates bunch slices from the collimator to the diagnostic station. One could therefore argue that particle dynamics in each slice during this operation is somehow different form that of the entire bunch. In the following paragraphs, we try to shed a light on this argument.

In the transverse plane, beam optical parameters may be affected by spurious dispersion and optical aberrations. These are single particle effects, thus independent from the longitudinal structure of the particles' ensemble. Collective effects like coherent synchrotron radiation (CSR) and geometric wakefields (GWs), instead, depend on the bunch length. CSR-induced slice emittance growth is still a controversial issue and so far associated to beams near full compression, as shown in [14–16]. This consideration is supported by simulations of high charge beams (>800pC) [17, 18] whose longitudinal phase space after compression is far from the upright configuration and whose slice normalized emittance deviates from its value before compression by ~0.1 μm.

CSR is often associated to the longitudinal space charge (LSC) in the context of microbunching instability. The instability gain as predicted by the linear theory is normally peaked at (uncompressed) wavelengths in the range 1–10 μm and often negligible at wavelengths longer than a few tens of micron [19, 20]. Thus, microbunching instability is not changing for slices longer than tens of micron.

Geometric wakefields induce linear and nonlinear distortion of the particle distribution in the (z,E) phase space, (z,x) and (z,y) physical plane. For very short bunches (i.e., slices), however, the wakefields' effect does depend on the bunch charge only. They are therefore suppressed by the few pC slice charge after collimation. In conclusion, beam collimation for femtosecond bunch slicing allows reliable 6-dimensional slice diagnostics. We estimate that slices with charge in the range <100 pC and duration in the range 10–100 fs suppress the effect of geometric wakefields in the RF linac. Particle dynamics related to optical aberrations and microbunching instability does not substantially change with respect to transport of the entire bunch, because they act on a length scale much smaller than the slice length. CSR-induced slice transverse emittance growth can be neglected for scenarios far from full magnetic bunch length compressions (upright longitudinal phase space).

OUTLOOK

The proposed beam collimation system offers an alternative way to diagnose slice properties of an electron bunch, with minimal impact on the machine configuration. A comparison of the performance of proposed scheme with other established techniques, such as RF deflecting cavities, is already in the authors' plan and will be faced in a dedicated work.

The proposed scheme extends the capability of a soft X-ray FEL facility to generate stable femtosecond pulses with tunable duration driven either by self-amplified spontaneous emission or an external seed laser. It is not straightforward to extend the proposed method to the generation of sub-femtosecond pulses as well as to hard X-ray FELs as both these scenarios would imply an electron charge at the level of a few pC in the delivery system. Electron beam diagnostics like BPMs might be appositely tuned to handle such a small signal level. We note, however, that a very low charge option is already on the horizon of existing and planned FEL facilities [21–24], thus anticipating a fundamental step forward for linac-based, short pulse FELs in the near future.

ACKNOWLEDGEMENT

The authors acknowledge L. Giannessi for the guidance to the code PERSEO and M. Cornacchia for numerous suggestions.

REFERENCES

[1] S. Di Mitri, D. Castronovo, I. Cudin, L. Fröhlich., Phys. Rev. Special Topics - Accel. Beams 16, 042801 (2013)
[2] C. J. Bocchetta, et al., FERMI@Elettra FEL Conceptual Design Report, </http://www.elettra.trieste.it/FERMI> (2007)
[3] E. Allaria, et al., Nat. Phot. 6, 699 (2012)
[4] P. Emma, K. Bane, M. Cornacchia, Z. Huang, H. Schlarb, G. Stupakov, and D. Walz, Phys. Rev. Lett. **92**, 074801 (2004)
[5] M. G. Minty and F. Zimmermann, Report No. SLAC-R-621 (2003)
[6] S. Di Mitri, E. M. Allaria, P. Craievich, W. Fawley, L. Giannessi, A. Lutman, G. Penco, S. Spampinati, and M. Trovo', Phys. Rev. ST Accel. and Beams **15**, 020701 (2012)

ISBN 978-3-95450-127-4

[7] P. Tenenbaum, K.L.F. Bane, L. Eriksson, J. Irwin, R.K. Jobe, D. McCormick, C.K. Ng, T.O. Raubenheimer, M.C. Ross, G. Stupakov, D. Walz, D. Onoprienko, and I. Zagorodnov, Phys. Rev. ST Accel. and Beams **10**, 034401 (2007).

[8] S. Di Mitri, L. Fröhlich, and E. Karantzoulis, Phys. Rev. ST Accel. and Beams **15**, 061001 (2012).

[9] E.D. Courant and H.S. Snyder, Annals of Phys. **3** 1 (1958). See also: S.Y. Lee, *Accelerator Physics*, published by World Scientific Publishing Co. Pte. Ltd., reprinted 2007, ISBN-13 978-981-256-182-4

[10] P. Craievich, S. Di Mitri and A. A. Zholents, Nucl. Instrum. Methods Phys. Res., Sect. A 604, 457 (2009)

[11] L.H. Yu, Phys. Rev. A 44, 5178 (1991)

[12] L.H. Yu *et al.*, Science 289, 932 (2000)

[13] L. Giannessi, in Proceedings of the 28th Free Electron Laser Conference, p. 91, Berlin, Germany (2006) http://www.afs.enea.it/gianness/perseo/

[14] M. Dohlus and T. Limberg, in Proc. of Part. Accel. Conf. 2005, Knoxville, Tennessee, USA (2005), TOAT006

[15] T. Limberg et al., in Proc. of Part. Accel. Conf. 2005, Knoxville, Tennessee, USA (2005), RPPT011

[16] P. Williams, "Design Options for the New Light Source", ASTeC Seminar (2008) http://www.cockroft.ac.uk/events/eslsxvi/nlswilliams

[17] S. Di Mitri, et al., NIM A 608, 19-27 (2009)

[18] M. Dohlus, in Proc. of 11th Intern. Comput. Accel. Physics Conf., Rostock-Warnemunde, Germany (2012), WEMPMP01

[19] Z. Huang et al., Phys. Rev. ST Accel. and Beams 7, 074401 (2004)

[20] M. Venturini, Phys. Rev. ST Accel. and Beams 10, 104401 (2007)

[21] Y. Ding, *et al.*, Phys. Rev. Lett. 102, 254801 (2009)

[22] S.V. Benson, D.R. Douglas, P. Evtushenko, F.E. Hannon, C. Hernandez-Garcia, J.M. Klopf, R.A. Legg, G.R. Neil, M.D. Shinn, C.D. Tennant, S. Zhang, and G.P. Williams, J. Modern Opt. 58, 16 (2011)

[23] *Swiss FEL Conceptual Design Report*, Ed. R. Ganter, PSI Bericht 10-04 (2010) http://www.psi.ch/swissfel/HomeEN/SwissFEL_CDR_web_small.pdf

[24] J.B. Rosenzweig et al., Nucl. Instrum. Methods Phys. Res., Sect. A 593, 39 (2008)

ISBN 978-3-95450-127-4